# Visualization of shock shapes around blunt bodies at hypersonic Mach number in a shock tunnel using electrical discharge technique

**K. Nagashetty, K. Syed Saifuddin, S. Saravanan, K. S. Gurumurthy\*, G. Jagadeesh# and K. P. J. Reddy†**

Department of Aerospace Engineering, Indian Institute of Science, Bangalore 560 012, India
*Department of Electronics and Computer Science, UVCE, Bangalore University, Bangalore 560 001, India
#SWRC, Institute of Fluid Science, Tohoku University, Sendai 980-8577, Japan

The flowfield around large angle blunt cones flying at hypersonic Mach numbers is complex with a strong detached shock wave in front. Visualization of these shock waves around the test models in ground-based testing facilities is an essential part of the modern day research in hypersonic aerodynamics. Recently we reported a technique based on electrical discharge to visualize the shock waves around bodies with simple geometries in a hypersonic shock tunnel. Extension of this technique for the visualization of shock shapes around a slender cone with blunt nose and a 120° apex angle blunt cone at zero and 45° angle of attack in HST2 shock tunnel with free stream Mach number of 5.75 is reported here. The strong shock wave ahead of the 120° apex angle blunt cone at zero incidence is compared with the theoretically estimated shock shape using a CFD code.

RECENTLY we reported a new technique for visualization of the flowfields around test models in a hypersonic shock tunnel[1]. This technique, based on the electrical discharge through the flowfields around the test model, differs from the conventional visualization techniques such as schlieren techniques, interferometry and holography. Most important aspect of the electrical discharge technique is the absence of any optical components and insensitivity to mechanical vibrations. Hence the technique can be employed for visualizing the flows even in harsher tunnel running conditions. In addition, the technique can be used for visualization of three-dimensional shock shapes around hypersonic test models[2].

We had reported flow visualization results using the electrical discharge technique for the simple body shapes like a flat plate and a slender cone in the hypersonic shock tunnel HST1 at IISc. The aim here is to report the visualization of shock waves around practical hypersonic vehicle shapes like blunt cones. The results reported here are obtained in the recently established hypersonic shock tunnel HST2. The experimentally visualized shock shape for a large angle blunt cone flying at hypersonic Mach number 5.75 is compared with the theoretical results predicted using a commercial CFD code.

The schematic diagram of HST2 shock tunnel along with the electrical circuit used for the generation of discharge across the flowfield is shown in Figure 1. The stainless steel shock tube of 50 mm internal diameter is capable of producing reservoir enthalpy ~5 MJ/kg at the entrance of the hypersonic nozzle in the reflected mode. The conical nozzle of 30 cm exit diameter produces freestream Mach number of 5.75 in 30 cm × 30 cm size test section. The test model along with the electrical connections is fixed in the test section using a bow-string arrangement with provision for changing the angle of attack.

The electrical discharge is generated inside the test section using a point-line electrode pair arrangement. The point electrode is suspended from the roof of the test section such that the disturbances generated due to the hypersonic flow over this electrode are not impinging on the test model. The line electrode is a thin (~0.2 mm) copper strip mounted vertically on the model such that the edge of the electrode is flush with the surface of the model. Typical electrode arrangement for a large angle blunt cone is shown in Figure 2. The distance between the electrodes is maintained around 60 mm to ensure uniform illumination of the flowfields at moderate voltage levels. Extreme care is taken to insulate the shock tunnel from high voltages during the discharge and the models are fabricated using bakelite material to ensure insulation as well as to eliminate
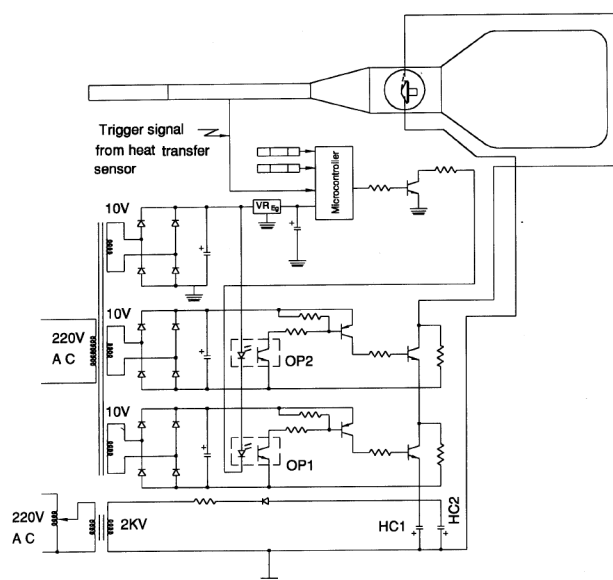


**Figure 1.** Schematic diagram of the hypersonic shock tunnel HST2 with the electrical circuit for flow visualization.
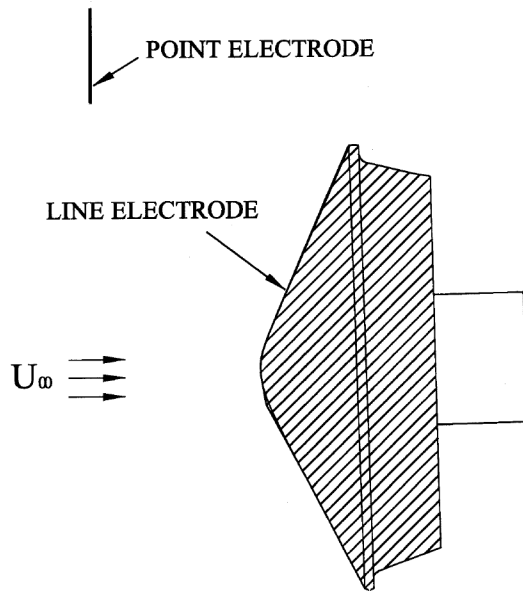
---

†For correspondence. (e-mail: laser@aero.iisc.ernet.in)

**Figure 2.** Point and line electrode arrangement used for generating electrical discharge over the large angle blunt cone model.
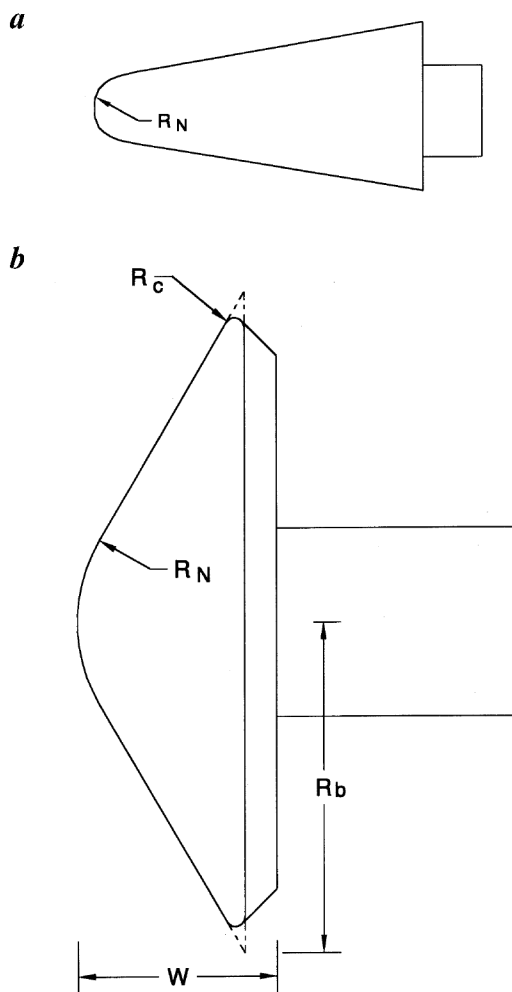




*a*

*b*

**Figure 3.** Schematic diagrams of (*a*) a slender cone with blunt nose and (*b*) a large angle blunt cone test models used for flow visualization in the shock tunnel.
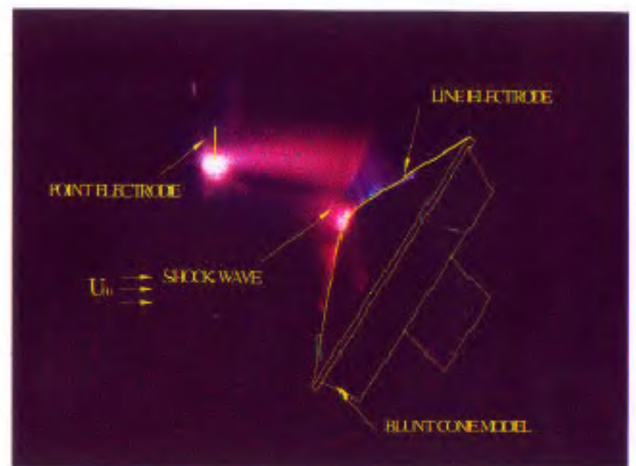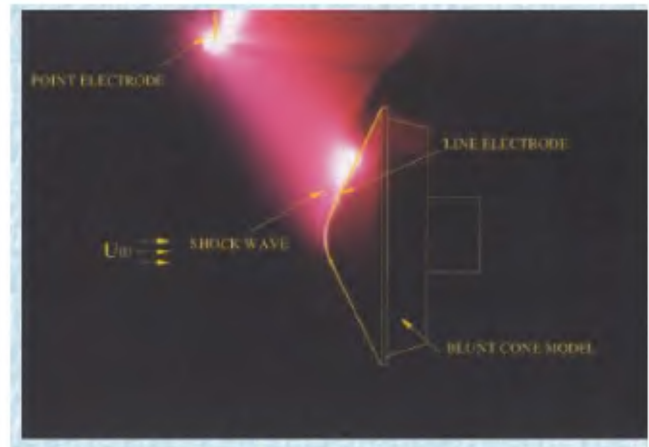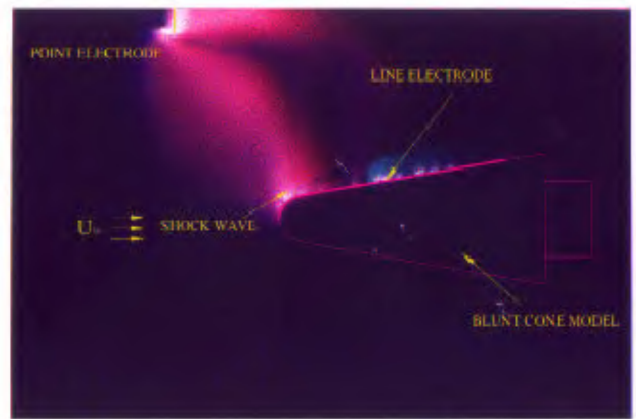


**Figure 4.** Detached shock waves in front of (*a*) slender cone with blunt nose, (*b*) large angle blunt cone at zero incidence and (*c*) large angle blunt cone at 45° angle of attack in Mach 5.75 hypersonic flow visualized using the electrical discharge technique.
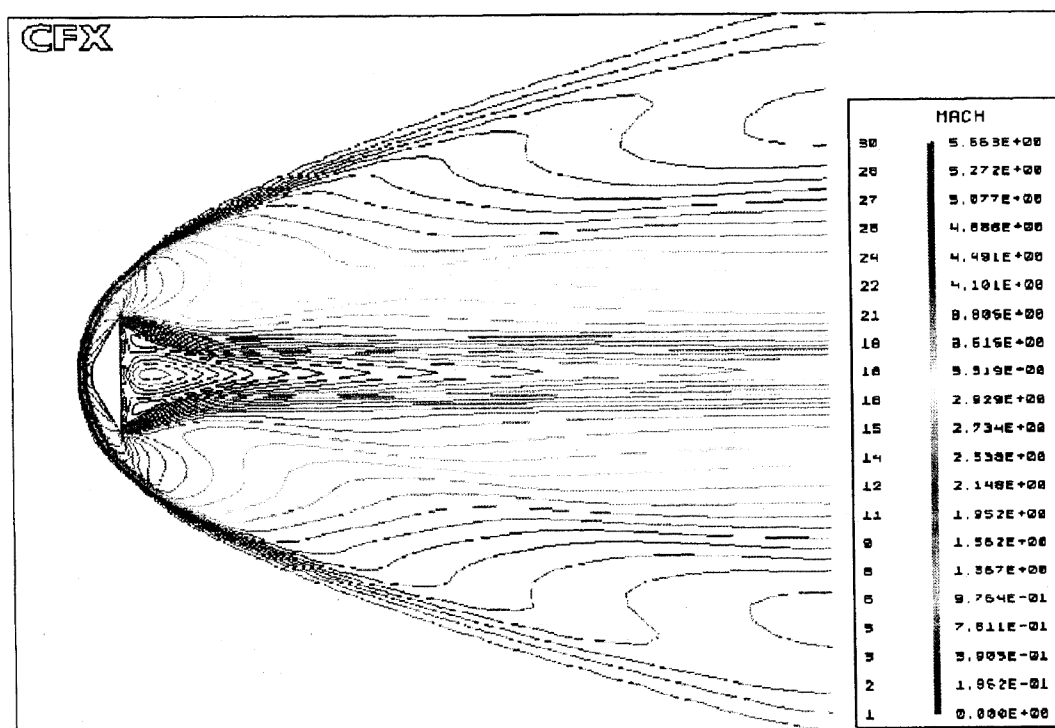
**Figure 5.** Mach contours generated using CFD code for 120° apex angle blunt cone at zero incidence in Mach 5.75 hypersonic flow.

reflection of stray light from the model surface. The details of the high voltage electrical power supply and the control circuit unit used for initiating and controlling the duration of the electrical discharge are given elsewhere[1].

The details of the models used in these experiments are shown schematically in Figure 3. The appropriate delay during the experiments is adjusted using the trigger signal from the thermal sensor near the end of the shock tube. The duration of the discharge is maintained at 2 μs and the light emitted by the electrical discharge is photographed using Olympus OM-2 model F1.8 camera in B exposure mode with a ASA 1600 film. The slender cone with blunt nose is used as a test case to establish the suitability of this technique for visualization of shock shapes for such class of bodies at hypersonic Mach numbers. The timing and the duration of the discharge were standardized with the help of this simple model before testing the complex models. The shock shapes around the slender cone with blunt nose, large angle (120° apex angle) blunt cone at zero and 45° of angle of attack in the hypersonic flow at Mach 5.75 are shown in Figure 4. These pictures show the detached bow shock wave in front of the hypersonic bodies and also the shock waves generated by the point electrode in the test section. It is clear from these pictures that the flow disturbances generated by the point electrode are not touching the model surface and the shock wave in front of the model is purely due to the

undisturbed hypersonic flow. The shock stand-off distance is clearly visible from these figures. Hence these figures can be used to study the variation of shock stand-off distance as a function of the binary scaling parameter (product of flow density and Reynolds number based on the blunt body radius) and the stagnation enthalpy.

We have also analysed the complex flowfields around the large angle blunt cone numerically using the commercial CFD code CFX-TASCflow (AEA International Plc.)[3,4]. This code solves the complete Navier–Stokes equations in the strong conservative form by an implicit pressure-based method. Coupled solutions of mass, momentum and energy are obtained using a novel finite element-based finite volume method. About 200 time steps were required for 4 orders of average residual reduction using the upwind differencing scheme which took approximately 10 h of CPU time on a RS5000 processor based Silicon Graphics workstation O2 running IRIX 6.3. The computed Mach contours of the Mach 5.75 hypersonic flow around the 120° apex angle blunt cone model are shown in Figure 5. The curved shock in front of the body has been well captured by the simulation. The shock wave visualized using the electrical discharge technique shown in Figure 4 matches very well with the numerically predicted shock shape for the 120° blunt cone at zero incidence. The measured stand-off distance of 6 mm compares well with the numerically predicted value.

1088

In conclusion, we have extended the electrical discharge-based flow visualization technique to visualize the flow fields around blunt cones in a hypersonic shock tunnel. The experimental results obtained in HST2 shock tunnel at IISc at a flow Mach number of 5.75 are compared with the numerically computed results for a 120° apex angle blunt cone. The visualized detached strong shock wave ahead of the body matches with predicted shock wave with a matching stand-off distance. The variation of shock stand-off distance as a function of the binary scaling parameter and the stagnation enthalpy is currently being investigated.

1. Jagadeesh, G., Srinivasa Rao, B. R., Nagashetty, K., Reddy, N. M. and Reddy, K. P. J., *Curr. Sci.*, 1996, **71**, 128–130.
2. Jagadeesh, G., Srinivasa Rao, B. R., Nagashetty, K., Reddy, N. M. and Reddy, K. P. J., *J. Flow Visualization Image Processing*, 1997, **4**, 51–57.
3. Jagadeesh, G., Reddy, N. M., Nagashetty, K. and Reddy, K. P. J., AIAA Paper 98-2601, June 1998.
4. Jagadeesh, G., Reddy, N. M., Nagashetty, K. and Reddy, K. P. J., *J. Spacecraft Rockets*, 2000, **37**, 137–139.

In conclusion, we have extended the electrical discharge-based flow visualization technique to visualize the flow fields around blunt cones in a hypersonic shock tunnel. The experimental results obtained in HST2 shock tunnel at IISc at a flow Mach number of 5.75 are compared with the numerically computed results for a 120° apex angle blunt cone. The visualized detached strong shock wave ahead of the body matches with predicted shock wave with a matching stand-off distance. The variation of shock stand-off distance as a function of the binary scaling parameter and the stagnation enthalpy is currently being investigated.

1. Jagadeesh, G., Srinivasa Rao, B. R., Nagashetty, K., Reddy, N. M. and Reddy, K. P. J., *Curr. Sci.*, 1996, **71**, 128–130.
2. Jagadeesh, G., Srinivasa Rao, B. R., Nagashetty, K., Reddy, N. M. and Reddy, K. P. J., *J. Flow Visualization Image Processing*, 1997, **4**, 51–57.
3. Jagadeesh, G., Reddy, N. M., Nagashetty, K. and Reddy, K. P. J., AIAA Paper 98-2601, June 1998.
4. Jagadeesh, G., Reddy, N. M., Nagashetty, K. and Reddy, K. P. J., *J. Spacecraft Rockets*, 2000, **37**, 137–139.

# A pilot study on the use of autofluorescence spectroscopy for diagnosis of the cancer of human oral cavity

**S. K. Majumder\*, S. K. Mohanty\*, N. Ghosh\*, P. K. Gupta\*,‡, D. K. Jain† and Fareed Khan†**

Biomedical Applications Section, Centre for Advanced Technology, Indore 452 013, India
†Department of Surgery, M. Y. Hospital, Indore 452 001, India

**The results of a pilot study to evaluate the potential of autofluorescence spectroscopy for the diagnosis of the cancer of oral cavity are presented. The study was carried out using a N₂ laser-based system developed in-house and involved 25 patients with histopathologically confirmed squamous cell carcinoma of oral cavity. A general multivariate statistical algorithm was developed to analyse and extract clinically useful information from the oral tissue spectra acquired *in vivo*. The algorithm could differentiate, over the sample size investigated, the squamous cell carcinoma of the oral cavity from normal squamous tissue with a sensitivity and specificity of 86% and 63%, respectively towards cancer. The relatively poor specificity is presumably because most of the patients investigated had advanced cancers, due to which some of the visually uninvolved sites treated as normal may not be truly normal.**

ORAL cancer is one of the most common cancers in India and several other South Asian countries and its incidence is on a rise due to consumption of tobacco and pan masala. There is, therefore, a growing need to develop sensitive and less invasive methods for screening cancerous or precancerous conditions of oral cavity.

Considerable work has been carried out on the use of laser-induced fluorescence (LIF) from native tissues for diagnosis of cancer[1–4]. This technique has the potential to probe *in situ* and quantitatively the biochemical changes that occur, as the tissue becomes neoplastic. Although LIF technique is particularly well suited for early detection of the cancer of oral cavity, due to easy accessibility of this organ, the evaluation of this diagnostic modality has not received requisite attention. In an earlier study on tissues of the oral cavity resected at biopsy[5], we found significant differences in the fluorescence signatures of malignant and normal sites. Based on the spectrally integrated intensity alone as the discrimination parameter, a sensitivity and specificity of ~90% was obtained in this study involving 47 patients.

In this communication, we report the results of a pilot study on 25 patients with histopathologically confirmed squamous cell carcinoma (SCC) of the oral cavity. A general multivariate statistical algorithm was developed to analyse and extract clinically useful information from the oral tissue spectra acquired *in vivo*. The algorithm could differentiate the SCC of the oral cavity from normal squamous tissues with a sensitivity and specificity towards cancer, of 86% and 63%, respectively. The relatively poor specificity is presumably because most of the patients investigated had advanced cancers, due to which some of the visually uninvolved sites treated as normal may not be truly normal.

A schematic of the N₂ laser-based portable fluorimeter developed for *in vivo* clinical studies is shown in Figure 1. It consists of a sealed-off N₂ laser (7 ns, 80 μJ, 10 Hz), a spectrograph coupled to a gateable intensified CCD camera (4 Quik 05A, Stanford Computer Optics Inc, USA) and a fiber optic probe to excite and collect fluorescence from the tissue. The probe, developed in-house, is an optical fiber bundle with two legs; one contains a single quartz fiber (NA 0.22, core diameter 400 μm) and the other contains six quartz fibers (NA 0.22, core diameter 400 μm). The two legs merge to form a common fiber bundle which consists of a central fiber, surrounded by a circular array of six fibers. The central fiber delivers excitation light to the tissue surface and the six surrounding fibers collect tissue